

NASA/CR-2014-218439



Range-specific High-Resolution Mesoscale Model Setup: Data Assimilation

Leela R. Watson

ENSCO, Inc., Cocoa Beach, Florida

NASA Applied Meteorology Unit, Kennedy Space Center, Florida

September 2014

NASA STI Program ... in Profile

Since its founding, NASA has been dedicated to the advancement of aeronautics and space science. The NASA scientific and technical information (STI) program plays a key part in helping NASA maintain this important role.

The NASA STI program operates under the auspices of the Agency Chief Information Officer. It collects, organizes, provides for archiving, and disseminates NASA's STI. The NASA STI program provides access to the NTRS Registered and its public interface, the NASA Technical Reports Server, thus providing one of the largest collections of aeronautical and space science STI in the world. Results are published in both non-NASA channels and by NASA in the NASA STI Report Series, which includes the following report types:

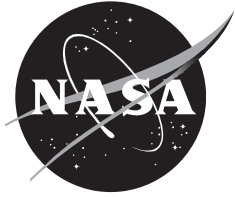
- **TECHNICAL PUBLICATION.** Reports of completed research or a major significant phase of research that present the results of NASA Programs and include extensive data or theoretical analysis. Includes compilations of significant scientific and technical data and information deemed to be of continuing reference value. NASA counterpart of peer-reviewed formal professional papers but has less stringent limitations on manuscript length and extent of graphic presentations.
- **TECHNICAL MEMORANDUM.** Scientific and technical findings that are preliminary or of specialized interest, e.g., quick release reports, working papers, and bibliographies that contain minimal annotation. Does not contain extensive analysis.
- **CONTRACTOR REPORT.** Scientific and technical findings by NASA-sponsored contractors and grantees.
- **CONFERENCE PUBLICATION.** Collected papers from scientific and technical conferences, symposia, seminars, or other meetings sponsored or co-sponsored by NASA.
- **SPECIAL PUBLICATION.** Scientific, technical, or historical information from NASA programs, projects, and missions, often concerned with subjects having substantial public interest.
- **TECHNICAL TRANSLATION.** English-language translations of foreign scientific and technical material pertinent to NASA's mission.

Specialized services also include organizing and publishing research results, distributing specialized research announcements and feeds, providing information desk and personal search support, and enabling data exchange services.

For more information about the NASA STI program, see the following:

- Access the NASA STI program home page at <http://www.sti.nasa.gov>
- E-mail your question to help@sti.nasa.gov
- Phone the NASA STI Information Desk at 757-864-9658
- Write to:
NASA STI Information Desk
Mail Stop 148
NASA Langley Research Center
Hampton, VA 23681-2199

NASA/CR-2014-218439



Range-specific High-Resolution Mesoscale Model Setup: Data Assimilation

Leela R. Watson

ENSCO, Inc., Cocoa Beach, Florida

NASA Applied Meteorology Unit, Kennedy Space Center, Florida

National Aeronautics and
Space Administration

*Kennedy Space Center
Kennedy Space Center, FL 32899-0001*

September 2014

Acknowledgments

The author thanks Mr. Brad Zavodsky of NASA's Short-term Prediction Research and Transition Center for providing the modeling scripts, data, and technical support throughout this project.

Available from:

NASA Center for AeroSpace Information
7115 Standard Drive
Hanover, MD 21076-1320
443-757-5802

This report is also available in electronic form at

<http://science.ksc.nasa.gov/amu>

Executive Summary

Mesoscale weather conditions can have an adverse effect on space launch, landing, and ground processing at the Eastern Range (ER) in Florida and Wallops Flight Facility (WFF) in Virginia. During summer, land-water interactions across Kennedy Space Center (KSC) and Cape Canaveral Air Force Station (CCAFS) lead to sea and river breeze front formation, which can spawn deep convection that can hinder operations and endanger personnel and resources. Many other weak locally driven low-level boundaries and their interactions with the sea breeze front and each other can also initiate deep convection in the KSC/CCAFS area. All these subtle weak boundary interactions often make forecasting of operationally important weather very difficult at KSC/CCAFS during the summer. These convective processes often build quickly, last a short time (60 minutes or less), and occur over small distances, all of which also pose a significant challenge to the local forecasters. Surface winds during the transition seasons (spring and fall) pose the most difficulties for the forecasters at WFF. They also encounter problems forecasting convective activity and temperature during those seasons.

Global and national scale models cannot properly resolve important local-scale weather features at each location due to their horizontal resolutions being much too coarse. Therefore, a properly tuned model at a high resolution is needed to provide improved forecasting capability. To accomplish this, the ER and WFF supported the Applied Meteorology Unit (AMU) task to perform a number of sensitivity tests in order to determine the best model configuration for operational use at each of the ranges to best predict winds, precipitation, and temperature. That task was completed in January 2013. This task is a continuation of that work and will provide a recommended local data assimilation (DA) and numerical forecast model design optimized for the ER and WFF to support space launch activities and for local weather challenges at both ranges.

The AMU examined different model configurations by running the DA on varying grid resolutions and nesting configurations to determine the impact on model skill. Data assimilation is an important component in producing quality numerical weather prediction forecasts. The DA software chosen for this task was the Gridpoint Statistical Interpolation (GSI) system developed by the National Centers for Environmental Prediction. The NASA Short-term Prediction Research and Transition Center provided a set of Perl scripts that run both the GSI DA system and the Weather Research and Forecast (WRF) model in a compact system. The objective of the scripts is to provide an easy-to-use interface for users to be able to execute GSI and WRF.

The AMU assessed model skill by using an objective statistical analysis that included the mean error, root mean square error, and Pearson correlation coefficient. Precipitation forecasts were evaluated using the Method for Object-Based Diagnostic Evaluation, a technique developed at the National Center for Atmospheric Research. Results indicate that for both the ER and WFF, a triple nest configuration that had a 9-km outer, 3-km middle, and 1-km inner nest was the optimal model configuration for both ranges. However, a double-nest configuration (2-km outer and 0.67-km inner nest) performed the best in predicting precipitation over the ER. Being able to predict summertime convection over the ER is operationally important and, for this reason, the AMU believes the double-nest configuration can be used as an alternative optimal configuration over the ER.

Future work will provide real-time output of the GSI/WRF cycled runs on the AMU's Advanced Weather Interactive Processing System II workstations. The AMU will also explore running the system in a rapid-refresh mode and will explore ensemble modeling to further improve model output.

Table of Contents

Executive Summary	1
Table of Contents.....	2
List of Figures	3
List of Tables	4
1 Introduction.....	5
1.1 Phase I Range Modeling Work.....	5
1.2 Report Format and Outline.....	6
2 Data and Model Configuration	7
2.1 Data Assimilation Software	7
2.2 Observational Data Ingest.....	7
2.3 Model Configuration and Test Cases	7
2.4 NASA SPoRT Perl Scripts	11
3 Model Forecast Validation.....	13
3.1 Observational Data	13
3.2 MET Software	15
3.3 ER Results.....	17
3.4 WFF Results.....	22
4 Conclusions and Future Work.....	27
References	28

List of Figures

Figure 1.	Map of the ER showing the single 1-km (D01) model domain boundary (1 dom).....	9
Figure 2.	Map of the ER showing the nested 2-km outer (D01) and 0.67-km inner (D02) model domain boundaries (2 doms).....	9
Figure 3.	Map of the triple nest configuration showing the 9-km outer (D01), 3-km middle (D02 and D04), and 1-km inner (D03 and D05) model domain boundaries over the ER and WFF (5 doms).....	10
Figure 4.	Map of WFF showing the nested 4-km outer (D01) and 1.33-km inner (D02) model domain boundaries (2 doms).....	10
Figure 5.	Schematic showing the 12-hour pre-cycling that occurs in the GSI/WRF system. Text in green is the model initialization time, solid red arrows are the pre-cycle forecast, and red dashed arrows are the full model forecast. This figure is a recreation of a NASA SPoRT produced schematic.....	12
Figure 6.	Map of a sampling of the mesonet and METAR weather station locations over the ER and the surrounding areas from MADIS.	13
Figure 7.	Map of a sampling of the mesonet and METAR weather station locations over WFF and the surrounding areas from MADIS.	14
Figure 8.	Chart of the average hourly ME for the 12-hour forecast over the entire POR for a) wind speed, b) wind direction, c) temperature, d) dewpoint temperature, and e) MSLP from the three GSI/WRF configurations at the ER.....	18
Figure 9.	Chart of the average hourly RMSE for the 12-hour forecast over the entire POR for a) wind speed, b) wind direction, c) temperature, d) dewpoint temperature, and e) MSLP from the three GSI/WRF configurations at the ER.....	19
Figure 10.	Chart of the average hourly PCC for the 12-hour forecast over the entire POR for a) wind speed, b) temperature, c) dewpoint temperature, and d) MSLP from the three GSI/WRF configurations at the ER.....	20
Figure 11.	Chart of the average hourly a) centroid distance (km), b) area ratio, and c) total interest value from the three GSI/WRF configurations for each hour of the 12-hour forecast over the entire POR at the ER.....	21
Figure 12.	Chart of the average hourly ME for the 12-hour forecast over the entire POR for a) wind speed, b) wind direction, c) temperature, d) dewpoint temperature, and e) MSLP from the two GSI/WRF configurations at WFF.....	23
Figure 13.	Chart of the average hourly RMSE for the 12-hour forecast over the entire POR for a) wind speed, b) wind direction, c) temperature, d) dewpoint temperature, and e) MSLP from the two GSI/WRF configurations at WFF.....	24
Figure 14.	Chart of the average hourly PCC for the 12-hour forecast over the entire POR for a) wind speed, b) temperature, c) dewpoint temperature, and d) MSLP from the two GSI/WRF configurations at WFF.	25
Figure 15.	Chart of the average hourly a) centroid distance (km), b) area ratio, and c) total interest value from the two GSI/WRF configurations for each hour of the 12-hour forecast over the entire POR at WFF.....	26

List of Tables

Table 1. List of conventional and satellite observations that can be assimilated into GSI.....	8
--	---

1 Introduction

Mesoscale weather conditions can have an adverse effect on space launch, landing, and ground processing at the Eastern Range (ER) in Florida and Wallops Flight Facility (WFF) in Virginia. During summer, land-sea interactions across Kennedy Space Center (KSC) and Cape Canaveral Air Force Station (CCAFS) lead to sea breeze front formation, which can spawn deep convection that can hinder operations and endanger personnel and resources. Many other weak locally driven low-level boundaries and their interactions with the sea breeze front and each other can also initiate deep convection in the KSC/CCAFS area. Some of these other boundaries include the Indian River breeze front, Banana River breeze front, outflows from previous convection, horizontal convective rolls, convergence lines from other inland bodies of water such as Lake Okeechobee, the trailing convergence line from convergence of sea breeze fronts due to the shape of Cape Canaveral, frictional convergence lines from the islands in the Bahamas, convergence lines from soil moisture differences, convergence lines from cloud shading, and others. All these subtle weak boundary interactions often make forecasting of operationally important weather very difficult at KSC/CCAFS during the convective season (May-Oct). These convective processes often build quickly, last a short time (60 minutes or less), and occur over small distances, all of which also poses a significant challenge to the local forecasters who are responsible for issuing weather advisories, watches, and warnings. Surface winds during the transition seasons of spring and fall pose the most difficulties for the forecasters at WFF. They also encounter problems forecasting convective activity and temperature during those seasons. Therefore, accurate mesoscale model forecasts are needed to aid in their decision making.

Both the ER and WFF would benefit greatly from high-resolution mesoscale model output to better forecast a variety of unique weather phenomena. Global and national scale models cannot properly resolve important local-scale weather features at each location due to their horizontal resolutions being much too coarse. Therefore, a properly tuned model at a high resolution is needed to provide improved capability. This task is a multi-year effort in which the Applied Meteorology Unit (AMU) will tune the Weather Research and Forecasting (WRF) model individually for each range. The goal of the first year, the results of which are in this report, was to tune the WRF model based on the best model resolution and run time while using reasonable computing capabilities. To accomplish this, the ER and WFF supported the tasking of the AMU to perform a number of sensitivity tests in order to determine the best model configuration for operational use at each of the ranges to best predict winds, precipitation, and temperature (Watson 2013). This task is a continuation of that work and will provide a recommended local data assimilation (DA) and numerical forecast model design optimized for the ER and WFF to support space launch activities. The model will be optimized for local weather challenges at both ranges.

1.1 Phase I Range Modeling Work

In Phase I of this task, the ER and WFF supported the tasking of the AMU to perform a number of sensitivity tests in order to determine the best model configuration for operational use at each of the ranges to best predict winds, precipitation, and temperature. The goal of the first phase, the results of which are in Watson (2013), was to tune the WRF model based on the best model resolution and run time while using reasonable computing capabilities.

The AMU compared model forecasts for both the ER and WFF using different WRF model dynamical cores, grid configurations, and physical schemes to determine the impact on model skill. Different model configurations were tested by varying the dynamical core, grid spacing, domain size, and forecast length. This enabled the AMU to determine the optimal configuration that allowed for the largest domain size and highest resolution to capture unique weather phenomena with the shortest wall-clock run time. Once the configurations were chosen, the AMU varied the model physics to determine which produced the best forecasts. The WRF model

forecasts were validated using simple statistics that compared locally available observational surface and upper-air data to the forecast data. The objective statistical analysis included the model bias, mean error (ME), and the root mean square error (RMSE). Precipitation forecasts were compared to nationally available rainfall data using the Method for Object-Based Diagnostic Evaluation (MODE), a technique developed at the National Center for Atmospheric Research (NCAR).

The AMU ran test cases in the warm and cool seasons at the ER and for the spring and fall seasons at WFF. For both the ER and WFF, the Advanced Research WRF (ARW) core outperformed the Non-hydrostatic Mesoscale Model core. Results for the ER indicate that the Lin microphysical scheme and the Yonsei University (YSU) planetary boundary layer (PBL) scheme is the optimal model configuration for the ER. It consistently produced the best surface and upper air forecasts, while performing fairly well for the precipitation forecasts. Both the Ferrier and Lin microphysical schemes in combination with the YSU PBL scheme performed well for WFF in the spring and fall seasons.

1.2 Report Format and Outline

This report presents the findings from a study of local DA and numerical forecast model design optimized for the ER and WFF to support space launch and for predicting unique weather phenomena at the ER and WFF. This analysis examined different model configurations by running the DA on varying grid resolutions and nesting configurations to determine the impact on model skill. The AMU assessed model skill by using an objective statistical analysis that included the ME, RMSE, and Pearson correlation coefficient (PCC). Precipitation forecasts were evaluated using MODE. Section 2 describes the DA software, the observational data used in the study, the model configurations, and the NASA Short-term Prediction Research and Transition Center (SPoRT) supplied Perl scripts used to run the forecast system. Section 3 describes the forecast validation technique and the results for both the ER and WFF. Section 4 contains the conclusions and future work.

2 Data and Model Configuration

The important aspects of this study were choice of DA software, the observational data ingest, period of record (POR), the DA/model configurations, and the DA/modeling system Perl scripts supplied by SPoRT.

2.1 Data Assimilation Software

DA is an important component in producing quality numerical weather prediction forecasts. DA methods are used to create a best estimate of the state of the atmosphere at the forecast initial time using information from observations and a background model forecast. This is accomplished through the minimization of an objective function that measures the weighted distance of the analysis from the observations and the background model. The weights assigned to each term are based on the error characteristics of the observations and the background model (Kleist et al. 2009). This creates an initial state that more closely resembles the state of the atmosphere at the model initialization time.

The DA software chosen for this task was the Gridpoint Statistical Interpolation (GSI) system developed by the National Centers for Environmental Prediction (NCEP). The GSI system is a three-dimensional variational DA system that is a freely available, community system designed to be flexible, state-of-the-art, and can run efficiently on various parallel computing platforms. It can be applied to both regional and global applications.

2.2 Observational Data Ingest

GSI can ingest large quantities of atmospheric observations and has developed capabilities for data thinning, quality controlling, and satellite radiance bias correction (Wang 2010). Table 1 lists some of the conventional and satellite radiance/brightness temperature observations that GSI can assimilate.

Most of these observations are complex and many of them need to be reformatted into Binary Universal Form for the Representation of meteorological data (BUFR) format or quality controlled before being used by GSI. NCEP produces quality-controlled data in BUFR format, called PrepBUFR files that can be used directly in GSI. These freely available files were used for this task.

2.3 Model Configuration and Test Cases

The AMU determined the main model configuration from the first phase of the Range Modeling task. The ARW core was used with the Lin microphysical scheme and the YSU PBL scheme for both the ER and WFF. Although the AMU previous work found the optimal horizontal grid spacing for the ER was a 2-km outer and 0.67-km inner domain and a 4-km outer and 1.33-km inner domain for WFF, the AMU conducted additional testing on the optimal horizontal grid spacing once the DA was added. Specifically, different configurations were run to determine the impact on the forecasts of running the DA over differing grid resolutions. For the ER, the AMU ran three configurations:

- Single domain: 1-km domain in which the DA was run (referred to as '1 dom', Figure 1),
- Nested domain: 2-km outer and 0.67-km inner domain in which the DA was run on the outer 2-km domain (referred to as '2 doms', Figure 2),
- Triple nested domain: 9-km outer, 3-km middle, and 1-km inner domain on which the DA was run on the 9-km outer domain (referred to as '5 doms', Figure 3).

For WFF, the AMU ran two configurations:

- Nested domain: 4-km outer and 1.33-km inner domain in which the DA was run on the outer 4-km domain (referred to as '2 doms', Figure 4),
- Triple nested domain: 9-km outer, 3-km middle, and 1-km inner domain on which the DA was run on the 9-km outer domain (referred to as '5 doms', Figure 3).

All other parameters were the same for each model run.

Table 1. List of conventional and satellite observations that can be assimilated into GSI.		
Conventional observations		
<ul style="list-style-type: none"> • Radiosondes • Conventional aircraft reports • MODIS IR and water vapor winds • Surface land observations • Doppler radial velocities • SBUV ozone profiles, MLS (including NRT) ozone, and OMI total ozone • Wind profilers: US, JMA • Dropsondes • GEOS hourly IR and cloud top wind • GPS Radio occultation refractivity and bending angle profiles 	<ul style="list-style-type: none"> • Pibal winds • ASDAR aircraft reports • GMS, JMA, and METEOSAT cloud drift IR and visible winds • SSM/I wind speeds • VAD (NEXRAD) winds • SST • Doppler wind Lidar data • Tail Doppler Radar radial velocity and super-observation • METAR cloud observations • SSM/I and TRMM TMI precipitation estimates 	<ul style="list-style-type: none"> • Synthetic tropical cyclone winds • MDCARS aircraft reports • EUMETSAT and GOES water vapor cloud top winds • QuikScat, ASCAT and OSCAT wind speed and direction • GPS precipitable water estimates • Tropical storm VITAL • Radar radial wind and reflectivity Mosaic • PM2.5 • Surface ship and buoy observation
Satellite radiance/brightness temperature observations		
<ul style="list-style-type: none"> • SBUV: n17, n18, n19 • AIRS: aqua • MHS: metop-a, metop-b, n18, n19 • AMSRE: aqua • GOME: metop-a, metop-b, • ATMS: NPP 	<ul style="list-style-type: none"> • HIRS: metop-a, metop-b, n17, n19 • SSMI: f14, f15 • SNDR: g11, g12, g13 • OMI: aura • SEVIRI: m08, m09, m10 	<ul style="list-style-type: none"> • GOES_IMG: g11, g12 • AMSU-A: metop-a, metop-b, n15, n18, n19, aqua • AMSU-B: metop-b, n17 • SSMIS: f16 • IASI: metop-a, metop-b

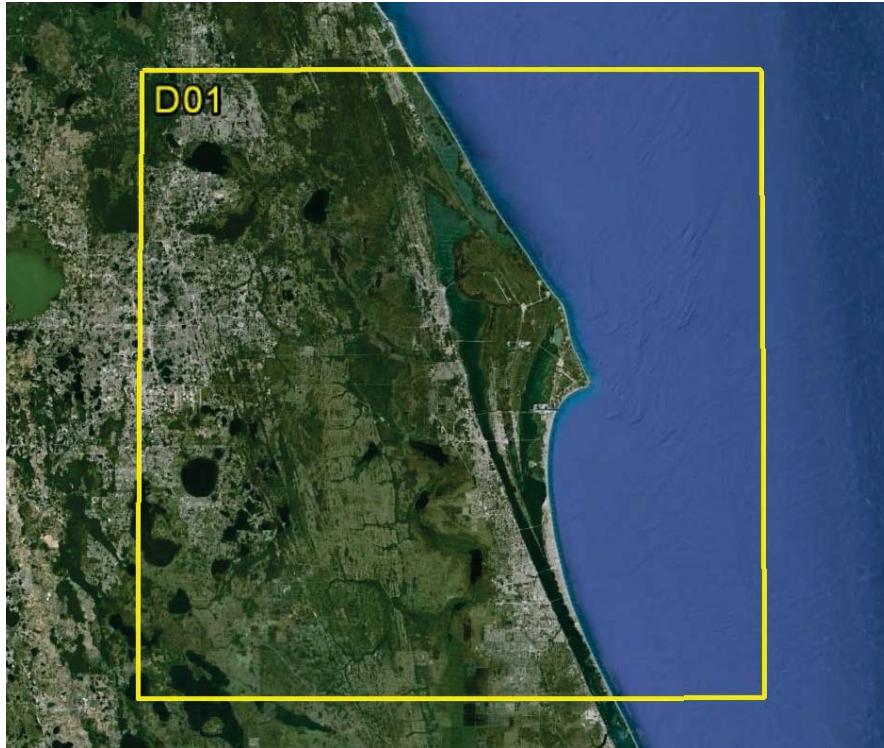


Figure 1. Map of the ER showing the single 1-km (D01) model domain boundary (1 dom).

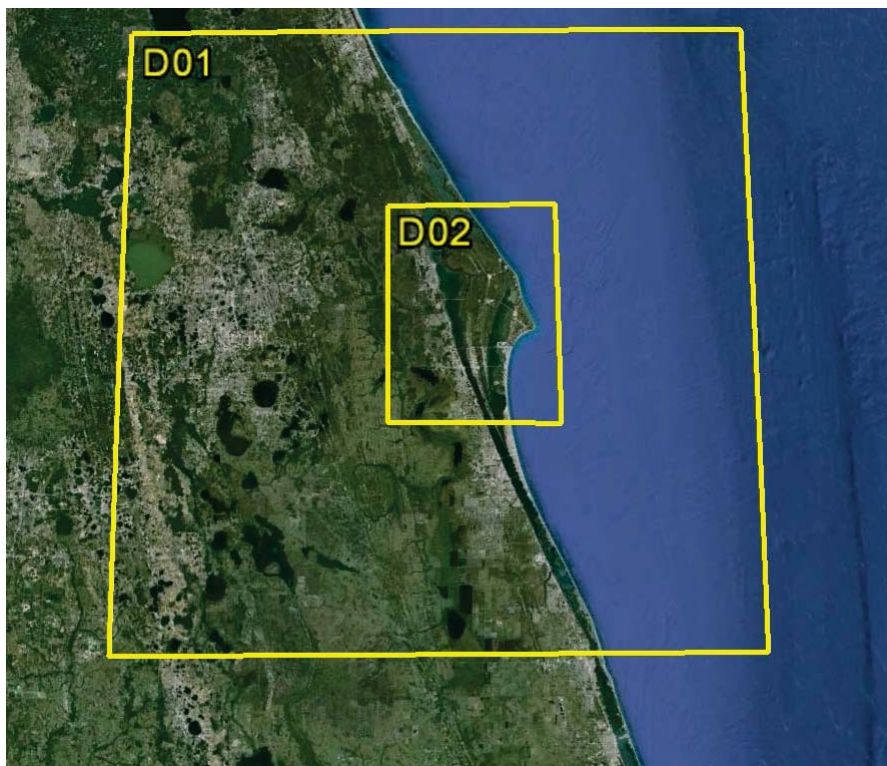


Figure 2. Map of the ER showing the nested 2-km outer (D01) and 0.67-km inner (D02) model domain boundaries (2 doms).

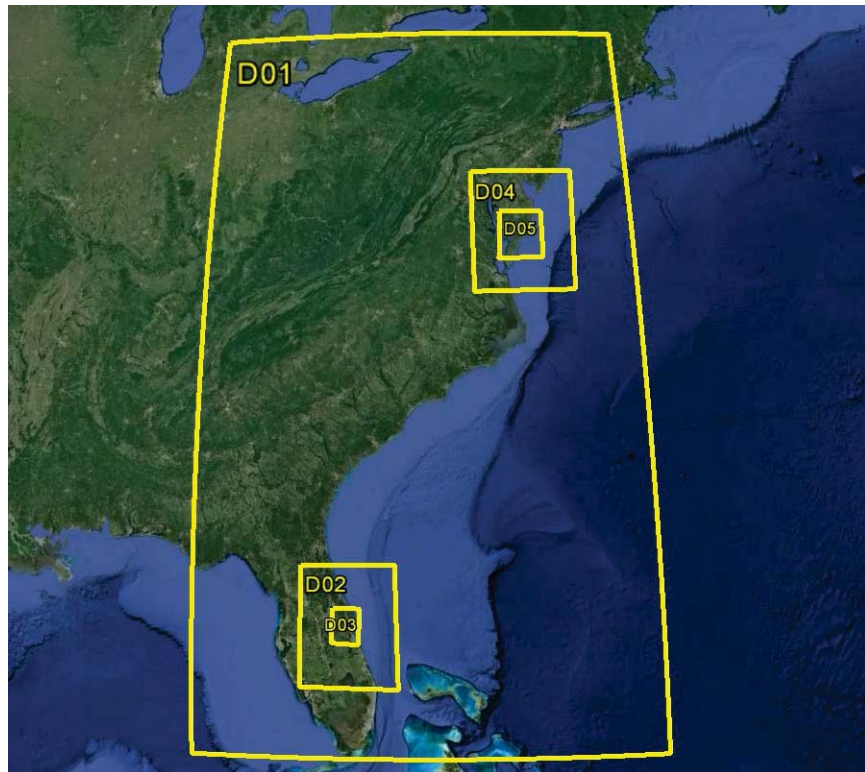


Figure 3. Map of the triple nest configuration showing the 9-km outer (D01), 3-km middle (D02 and D04), and 1-km inner (D03 and D05) model domain boundaries over the ER and WFF (5 doms).

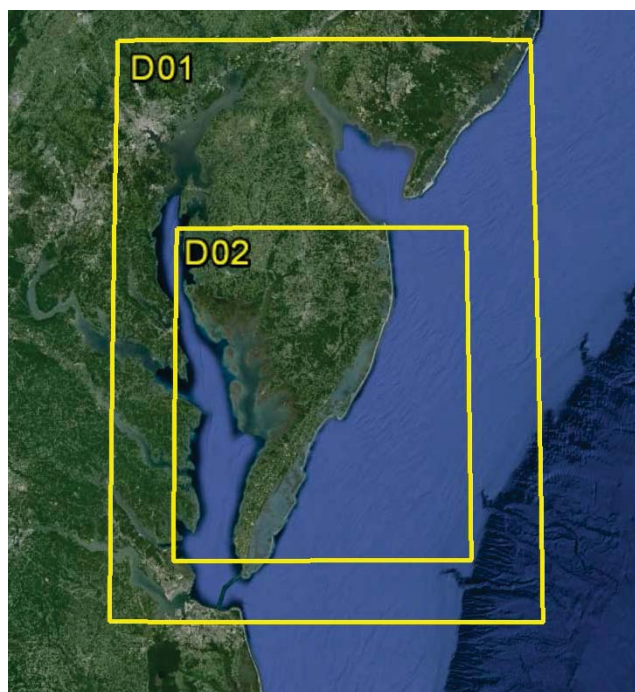


Figure 4. Map of WFF showing the nested 4-km outer (D01) and 1.33-km inner (D02) model domain boundaries (2 doms).

The AMU ran each DA/model simulation at the specified horizontal resolution with 35 irregularly spaced, vertical sigma levels up to 50 mb. Each run was initiated four times per day at 0000, 0600, 1200, and 1800 UTC and integrated 12 hours using the 13-km Rapid Refresh (RAP) model for boundary conditions and as the background model first-guess field, Land Information System (LIS) data from SPoRT for land surface data, and sea surface temperature (SST) data from both NCEP's Real-time Global SSTs and the SPoRT 2-km SST composites. Initial conditions were created using a cycled GSI/WRF approach that is described in Section 2.4. The POR for the test cases was from 1200 UTC 27 August 2013 to 0600 UTC 10 November 2013.

2.4 NASA SPoRT Perl Scripts

SPoRT provided a set of Perl scripts that run both the GSI DA system and the WRF model in a compact system. The objective of the scripts is to provide an easy-to-use interface for users to be able to execute GSI and WRF. The SPoRT scripts are simply a wrapper to support running of the software systems, which must be downloaded and installed separately by the user.

The GSI/WRF scripts use a cycled GSI system similar to the operational North American Mesoscale (NAM) model. The scripts run a 12-hour pre-cycle in which data are assimilated from 12 hours prior up to the model initialization time. This is done due to the time latency of the satellite data. Satellite data are not available instantaneously as it takes time to receive and process. If the pre-cycling did not occur, there would be very little influence on model output from the satellite observations, which have been shown to have the largest positive impact on most forecast systems. Once the pre-cycling is complete, a 12-hour forecast is run.

A schematic of the GSI/WRF pre-cycling system is shown in Figure 5. Model initialization times are shown in green, pre-cycle times are shown in blue, and forecasts are shown in red. As stated above, the model is run four times per day. For a model initialization time of 0000 UTC (t00Z in Figure 5), the GSI/WRF scripts are started between 0000 and 0100 UTC. The scripts begin their pre-cycling 12 hours prior to initialization time, in this case at 1200 UTC of the previous day. Initial conditions for the WRF forecast are first created by processing the RAP data as the background model, the LIS land surface data, and NCEP and SPoRT SST data using the WRF preprocessing system. Once a background grid has been established, observational data are assimilated into the background grid using the GSI system. After the observations have been assimilated, a 3-hour WRF forecast is run (red arrow between tm12 and tm09 for t00Z). The pre-cycle begins again using data from nine hours prior to the initialization time (tm09, 1500 UTC of the previous day), however, the 3-hour WRF forecast is now used as the background model for the next forecast. This process continues every three hours until the initialization time is reached. At 0000 UTC after the background grid is created using the 3-hour WRF forecast and the observational data is assimilated, a 12-hour WRF forecast is run (red dashed line). The process repeats itself every six hours.

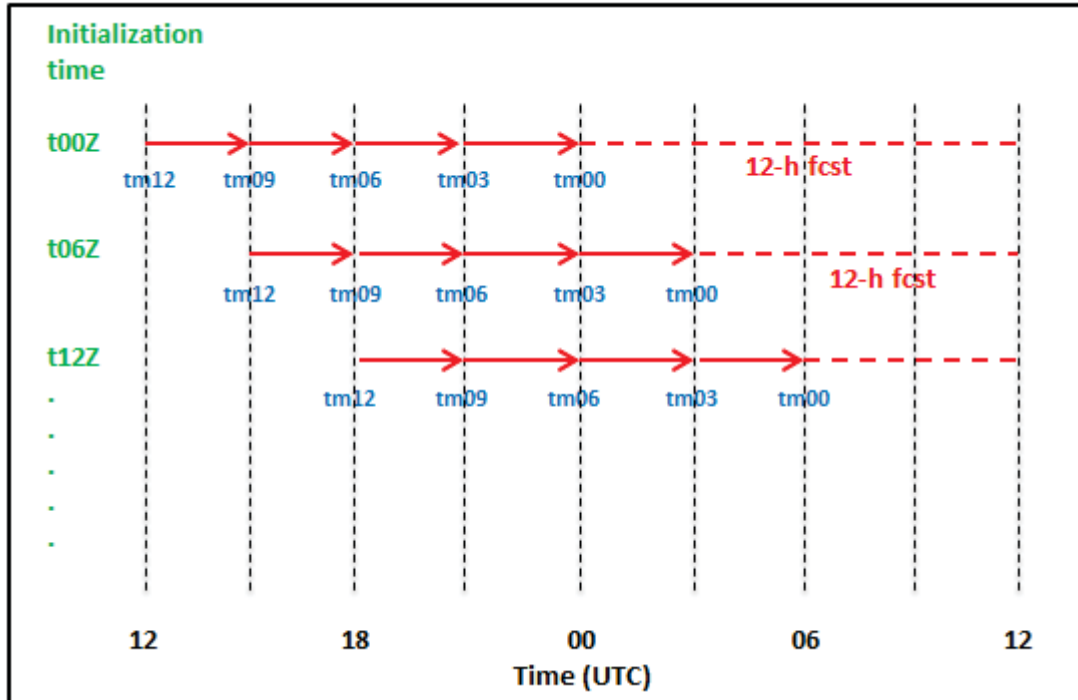


Figure 5. Schematic showing the 12-hour pre-cycling that occurs in the GSI/WRF system. Text in green is the model initialization time, solid red arrows are the pre-cycle forecast, and red dashed arrows are the full model forecast. This figure is a recreation of a NASA SPoRT produced schematic.

3 Model Forecast Validation

The AMU validated the GSI/WRF model forecasts using statistics that compared locally available surface observations to the forecast data. Precipitation forecasts were compared to nationally available rainfall data using a technique developed at NCAR.

3.1 Observational Data

In order to verify the GSI/WRF model performance, surface weather observations of temperature, dewpoint, wind speed and direction, and atmospheric pressure were required. NCEP's Meteorological Assimilation Data Ingest System (MADIS) and Stage IV precipitation data were used for the observational datasets.

MADIS was developed by NOAA's Earth System Research Laboratory Global Systems Division to collect, integrate, quality control, and distribute observations from a multitude of organizations. MADIS includes various meteorological surface datasets (such as Meteorological Aerodrome Report (METAR), maritime, and mesonet data, among others), profiler network data, aircraft data, radiosondes, satellite data, hydrological surface data, radiometer, and snow data.

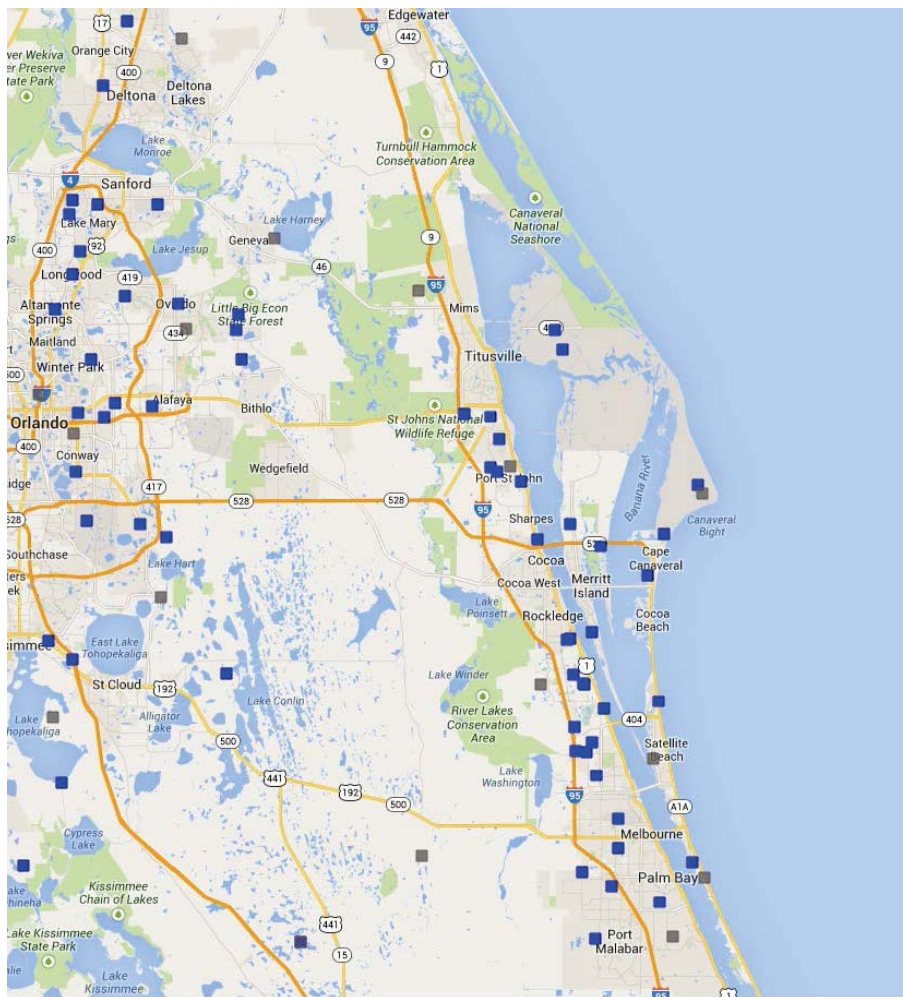


Figure 6. Map of a sampling of the mesonet and METAR weather station locations over the ER and the surrounding areas from MADIS.

For this task, the AMU downloaded METAR and mesonet data to validate the GSI/WRF forecasts. METAR is the international standard code format for hourly surface weather observations and typically contains data for the temperature, dew point, wind speed and direction, precipitation, cloud cover and heights, visibility, and barometric pressure. Mesonet data is a network of automated weather stations designed to observe mesoscale meteorological phenomena, such as dry lines, squall lines, and sea breezes, and report conditions in time intervals anywhere from 1 to 15 minutes. The locations of some of the METAR and mesonet stations over the ER and WFF are shown in Figure 6 and Figure 7, respectively.

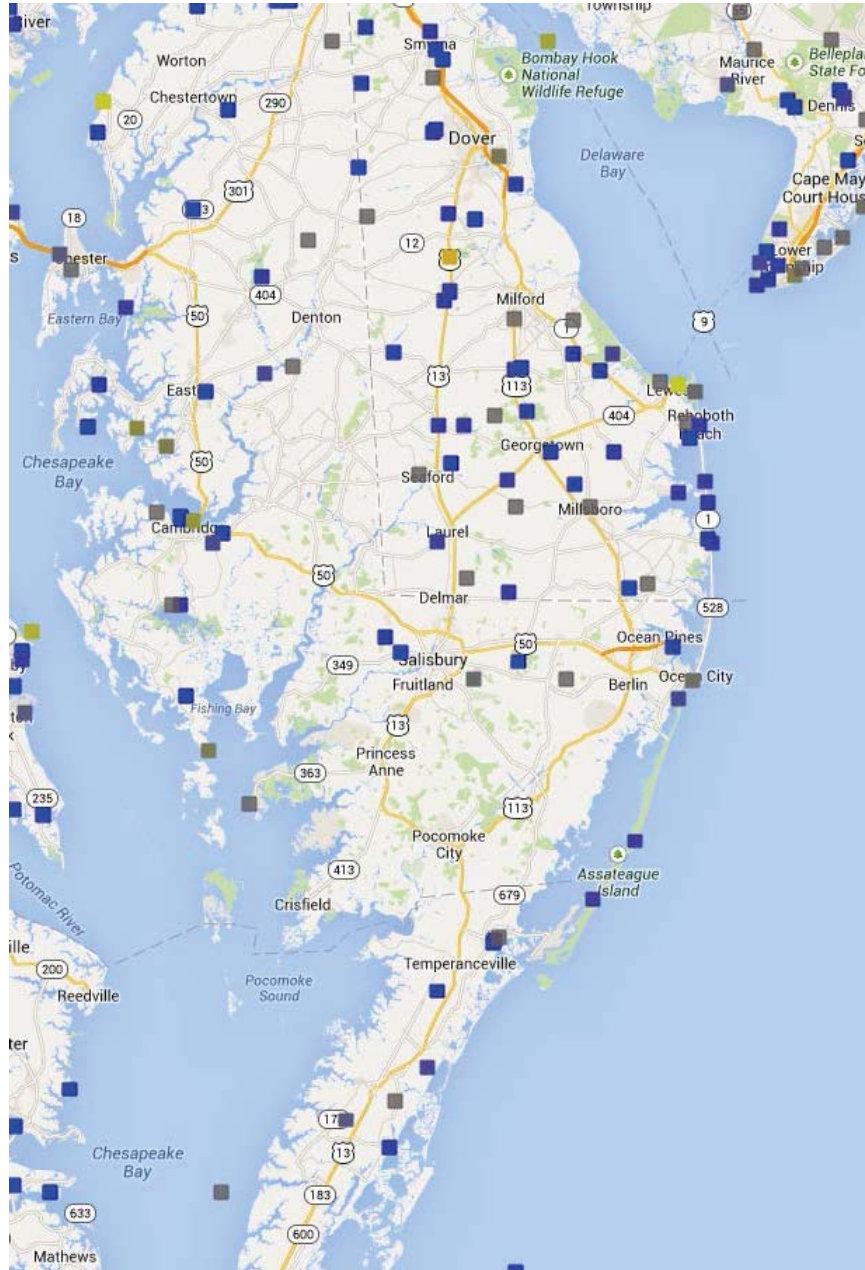


Figure 7. Map of a sampling of the mesonet and METAR weather station locations over WFF and the surrounding areas from MADIS.

To verify precipitation, the AMU compared hourly forecast rainfall accumulation to the NCEP Stage-IV analysis (<http://www.emc.ncep.noaa.gov/mmb/ylin/pcpanl/stage4/>). This analysis combines radar data and rain gauge reports to produce hourly rainfall accumulation on a 4-km grid. It is a manually quality-controlled continental U.S. mosaic from the regional 1-hour precipitation analyses produced by 12 National Weather Service River Forecast Centers (Lin and Mitchell 2005).

3.2 MET Software

For the objective analysis, the AMU compared observed wind speed, temperature, dewpoint temperature, mean sea-level pressure, and accumulated precipitation observations to the forecast variables using the latest version of the Model Evaluation Tools (MET) software. This software was developed by the NCAR Developmental Testbed Center. It is a state-of-the-art suite of verification tools that uses output from the WRF model to compute standard verification scores comparing gridded model data to point or gridded observations, and uses spatial verification methods comparing gridded model data to gridded observations using object-based decomposition procedures. For this task, two MET tools were chosen to validate the GSI/WRF forecasts: the Point-Stat tool and the MODE tool.

3.2.1 Point-Stat Tool

The MET Point-Stat tool was used to verify the surface forecasts. This tool provides verification statistics for forecasts at observation points, in this case, at the METAR and mesonet point observations. The Point-Stat tool matches gridded forecasts to point observation locations using a user-specified interpolation approach and computes the verification statistics.

Many output statistics are available within the Point-Stat tool. This study looked at three of those statistics for wind speed, temperature (T), dewpoint temperature (T_d), and mean sea-level pressure (MSLP): the ME, the RMSE, and the PCC; and two statistics for wind direction: the ME and the RMSE. The statistics compared all mesonet and METAR observations available to the corresponding locations in the model forecast output at a 1-hour interval.

The mean error, ME, is a measure of the overall bias of the model parameter being compared. A perfect forecast has ME = 0. It is defined as:

$$ME = \frac{1}{n} \sum_{i=1}^n (f_i - o_i)$$

where:

n = number of forecast and observation pairs over the forecast period,

f_i = WRF forecast of T, T_d , MSLP, wind speed, or wind direction, and

o_i = observed T, T_d , MSLP, wind speed, or wind direction.

The model RMSE was calculated to measure the magnitude of the error. It is useful in determining whether the forecasts produced large errors, as it gives relatively high weight to large errors. It is calculated using the following equations:

$$MSE = \frac{1}{n} \sum_{i=1}^n (f_i - o_i)^2$$

$$RMSE = \sqrt{MSE}$$

where n , f_i , and o_i are defined as above.

The PCC, r , measures the strength of the linear association between the forecast and observed parameters. It is defined as:

$$r = \frac{\sum_{i=1}^n (f_i - \bar{f})(o_i - \bar{o})}{\sqrt{\sum_{i=1}^n (f_i - \bar{f})^2 \sum_{i=1}^n (o_i - \bar{o})^2}}$$

where n , f_i , and o_i are defined as above and:

\bar{f} = average forecast over time and space of T, T_d, MSLP, wind speed, or wind direction, and

\bar{o} = average observed over time and space of T, T_d, MSLP, wind speed, or wind direction.

The PCC can range between -1 and 1 where 1 indicates a perfect correlation, -1 indicates a perfect negative correlation, and 0 indicates no correlation between the forecast and observations. For example, the PCC for wind speed measures whether large values of forecast wind speed tend to be associated with large values of observed wind speed (positive correlation), whether small values of forecast wind speed tend to be associated with large values of observed wind speed or vice versa (negative correlation), or whether values of both variables are unrelated (correlation near 0).

3.2.2 MODE

To verify precipitation, the AMU compared the forecast hourly rainfall accumulation to the observed rainfall over the same time period. MODE was used to determine the skill of each model configuration. MODE is an object-based verification system that compares gridded observations to gridded forecasts. It resolves and compares objects, such as areas of accumulated rainfall, in both the forecast and observed fields. The objects are described geometrically and then the attributes of the objects can be compared (Davis et al. 2006). MODE outputs statistics that describe the correlation between the objects and allows the user to identify forecast strengths or weaknesses. Details about how objects are identified and characterized can be found in Davis et al. (2006). For this report, the objects of interest are areas of accumulated rainfall. Therefore, references to objects are references to areas of resolved accumulated rainfall throughout the forecast period.

Once the objects have been identified, their various properties are evaluated and compared. The object attributes examined by the AMU in this task included the centroid distance, area ratio, and total interest value. The centroid distance is the vector difference between the centroids of the forecast and observed objects. It describes the location bias in the forecasts. The smaller the distance between the centroids, the better the forecast. The area ratio compares the area, or number of grid squares, the forecast object occupies compared to the observed object. An area ratio of 1 is considered a perfect correlation. Interest value is defined as the differences in particular attributes between the forecast and observed objects. Interest values of 0 indicate no interest, or a poor forecast, while a value of 1 indicates high interest, or a good forecast. The total interest value is a weighted sum of specific interest values and is used as an overall indicator of the quality of the precipitation forecast. Total interest value is large when forecast and observed objects are well correlated (are roughly the same size and are close to each other) and is small when they are not well correlated.

3.3 ER Results

The AMU validated model performance for the ER using forecasts from the grids described in section 2.3, where 2 doms references the nested 2-km outer and 0.67-km inner domain (Figure 2), 1 dom references the single 1-km domain (Figure 1), and 5 doms references the triple nested 9-km outer, 3-km middle, and 1-km inner domain over the ER (Figure 3).

3.3.1 Surface Forecasts

The AMU validated the GSI/WRF forecasts with the local METAR and mesonet data. Figure 8 shows the ME for wind speed, wind direction, temperature, dewpoint temperature, and MSLP from the three GSI/WRF configurations averaged over each hour of each 12-hour forecast for the entire POR at the ER.

Overall, the ME results indicate that the triple-nest configuration performed the best of the three configurations, followed by the nested domain, and then the single domain. The triple-nest configuration had the lowest ME for wind speed, wind direction, dewpoint temperature, and MSLP while the nested domain had the lowest ME for temperature. The single domain had the highest ME for wind speed, temperature, and dewpoint temperature.

The average hourly ME results for wind speed indicated that all three domain configurations over-predicted the wind speed throughout the forecasts. The ME for wind speed for the single domain was approximately 2 m/s higher than for either nested domain during the entire forecast period with an average hourly ME of approximately 5 m/s. All three domains followed the same trend of slightly increasing ME throughout the forecasts for wind direction. The single domain had a consistent warm bias throughout the forecasts as indicated by the average hourly ME for temperature with a maximum ME of approximately 0.7 K. Both nested domains exhibited a cool bias throughout the forecasts, except for the 0-hour forecast. All domain configurations exhibited a cool dewpoint temperature bias, with the single domain showing the largest cool bias in the 2 to 2.3 K range. Results from the average hourly ME for MSLP show that all three configurations followed the same trend of an initial negative, or low pressure, bias followed by a slight positive, or high pressure, bias.

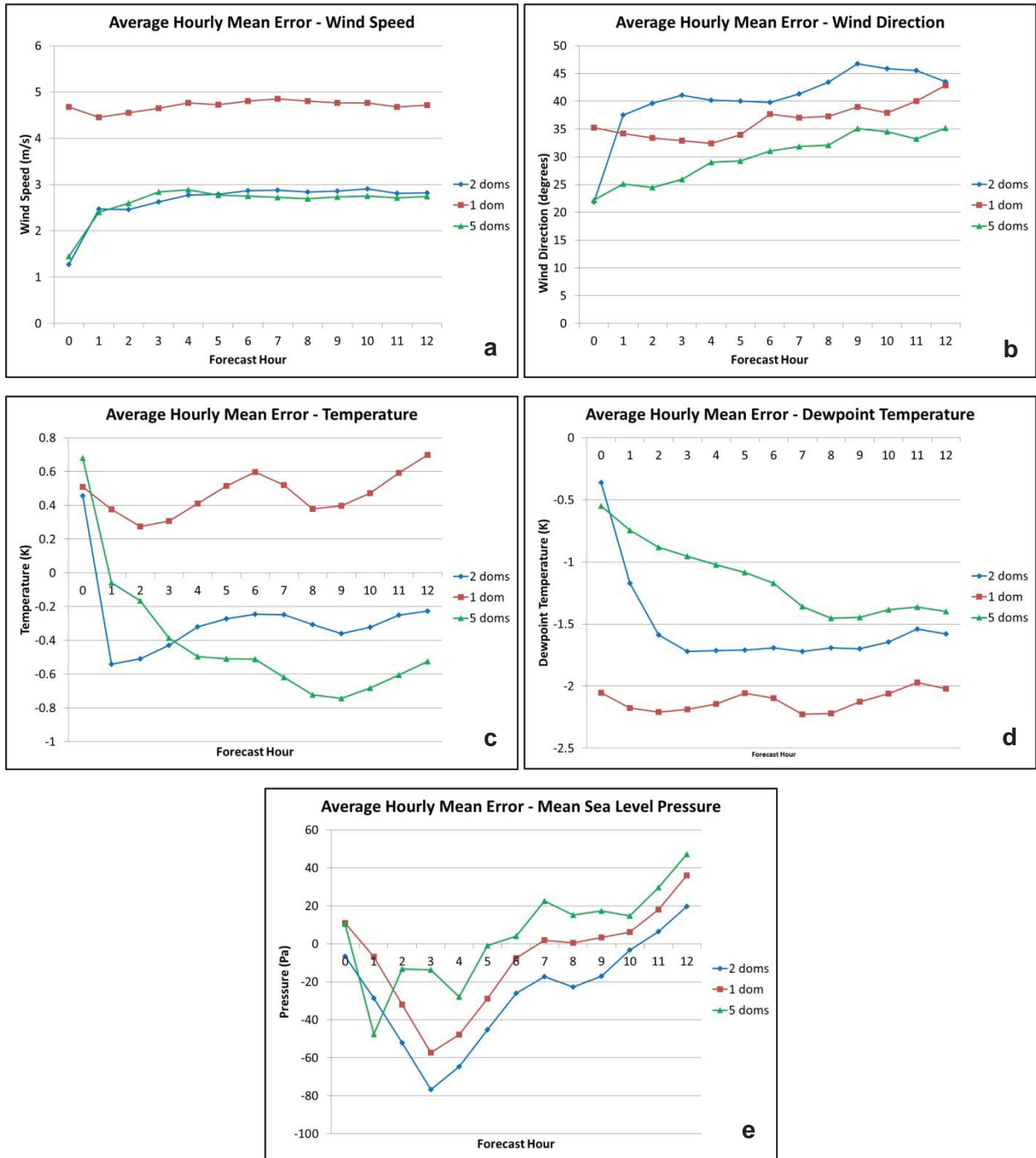


Figure 8. Chart of the average hourly ME for the 12-hour forecast over the entire POR for a) wind speed, b) wind direction, c) temperature, d) dewpoint temperature, and e) MSLP from the three GSI/WRF configurations at the ER.

As with ME, the RMSE results (Figure 9) indicate that the triple-nest configuration performed the best of the three configurations, followed by the nested domain, and then the single domain. The triple-nest configuration had the lowest RMSE for wind speed, wind direction, and dewpoint temperature while the nested domain had the lowest RMSE for temperature and MSLP. The single domain had the highest RMSE for all variables except wind direction.

The general trends for the average hourly RMSE for wind speed and direction are nearly the same as the ME. The RMSE for temperature and dewpoint temperature indicate that the single domain still performed the worst. Average hourly RMSE for MSLP results are similar to the ME results, with all three domain configurations showing nearly the same trends in RMSE throughout the forecast.

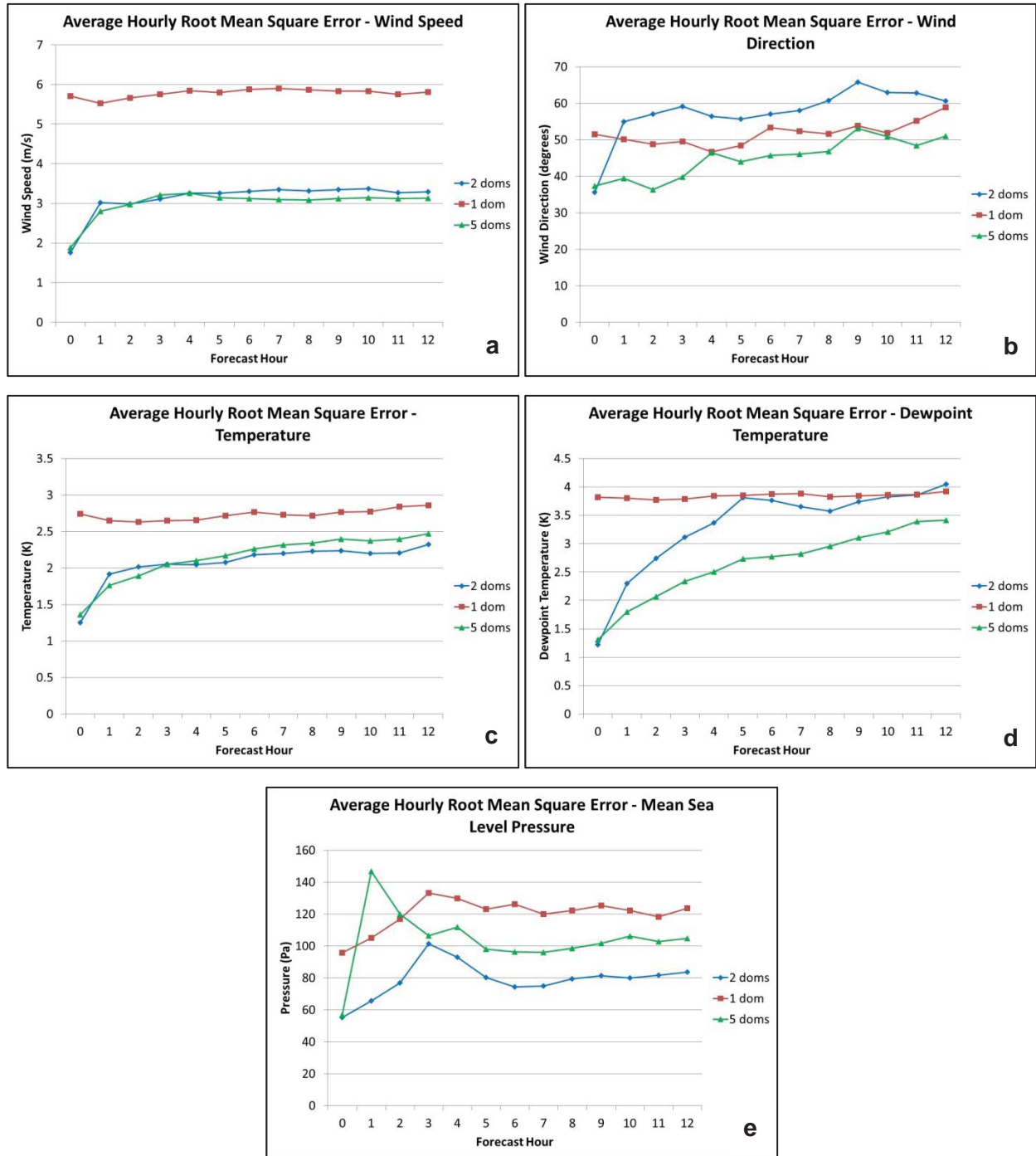


Figure 9. Chart of the average hourly RMSE for the 12-hour forecast over the entire POR for a) wind speed, b) wind direction, c) temperature, d) dewpoint temperature, and e) MSLP from the three GSI/WRF configurations at the ER.

The PCC can indicate whether the model configurations captured the overall trend of the observed variables. Using wind speed as an example, it answers the question of whether the model winds fluctuated positively and negatively with the same magnitude as the observed winds. The closer the PCC is to 1, the better the model was able to capture these trends. When comparing these particular forecast vs. observed variables, only positive coefficients indicate any value in the model forecasts.

The results from the PCC (Figure 10) calculation indicate that the triple-nested configuration again performed the best of the three configurations followed by the single domain and then the nested domain. The triple-nest configuration had the highest PCC for wind speed, temperature, and MSLP while the single domain had the highest PCC for dewpoint temperature.

All results show a positive correlation, except for the nested domain during forecast hours 8-9 for MSLP indicating that the fluctuations in each of the variables was captured by the model. However, overall the values for PCC were low. This may be due to the difficulty in capturing mesoscale phenomena in the summertime over the ER.

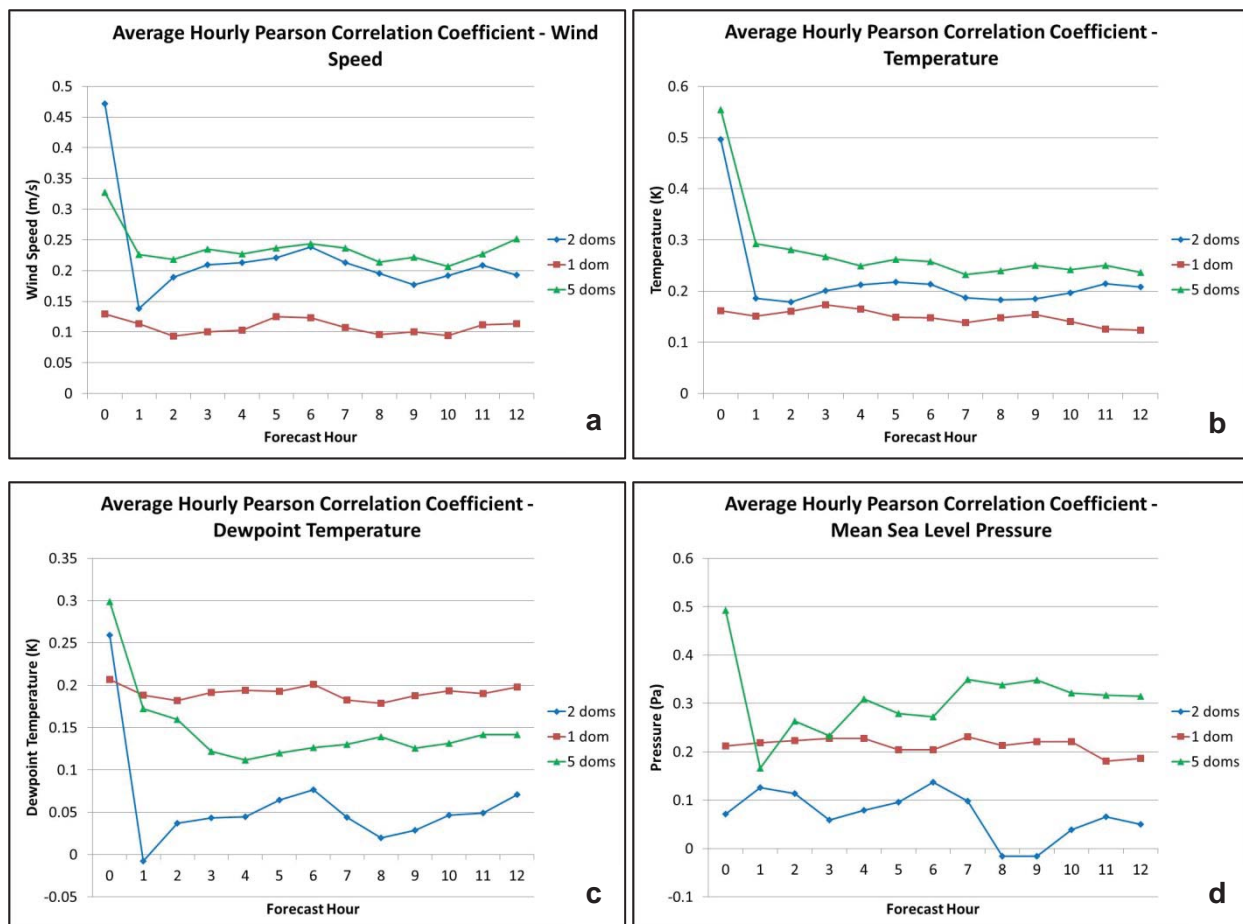


Figure 10. Chart of the average hourly PCC for the 12-hour forecast over the entire POR for a) wind speed, b) temperature, c) dewpoint temperature, and d) MSLP from the three GSI/WRF configurations at the ER.

3.3.2 Precipitation Forecasts

The AMU compared precipitation forecasts from all three model configurations to determine performance differences. One-hour forecast accumulated rainfall for each hour of each of the 12-hour forecasts was compared to the one-hour accumulation of observed rain using the NCEP Stage-IV analysis data for each day during the POR. The POR summary statistics for each hour of the forecast of centroid distance, area ratio, and total interest value from the MODE software are shown in Figure 11. The centroid distance (km) results indicate that the nested domain precipitation matched the location of the observed precipitation most closely throughout the forecasts, followed by the triple-nest configuration and then the single domain. The area ratio for the nested domain indicates that the forecast most closely matched the areal coverage of observed precipitation, with the triple-nest and single domain performing slightly worse and similarly, respectively. Interest value functions near 0.9 for the nested domain indicates that overall the forecast correlated the best with the observed precipitation, followed by the triple-nest configuration and then single domain. Overall, the nested domain outperformed both triple-nest and single domain configurations.

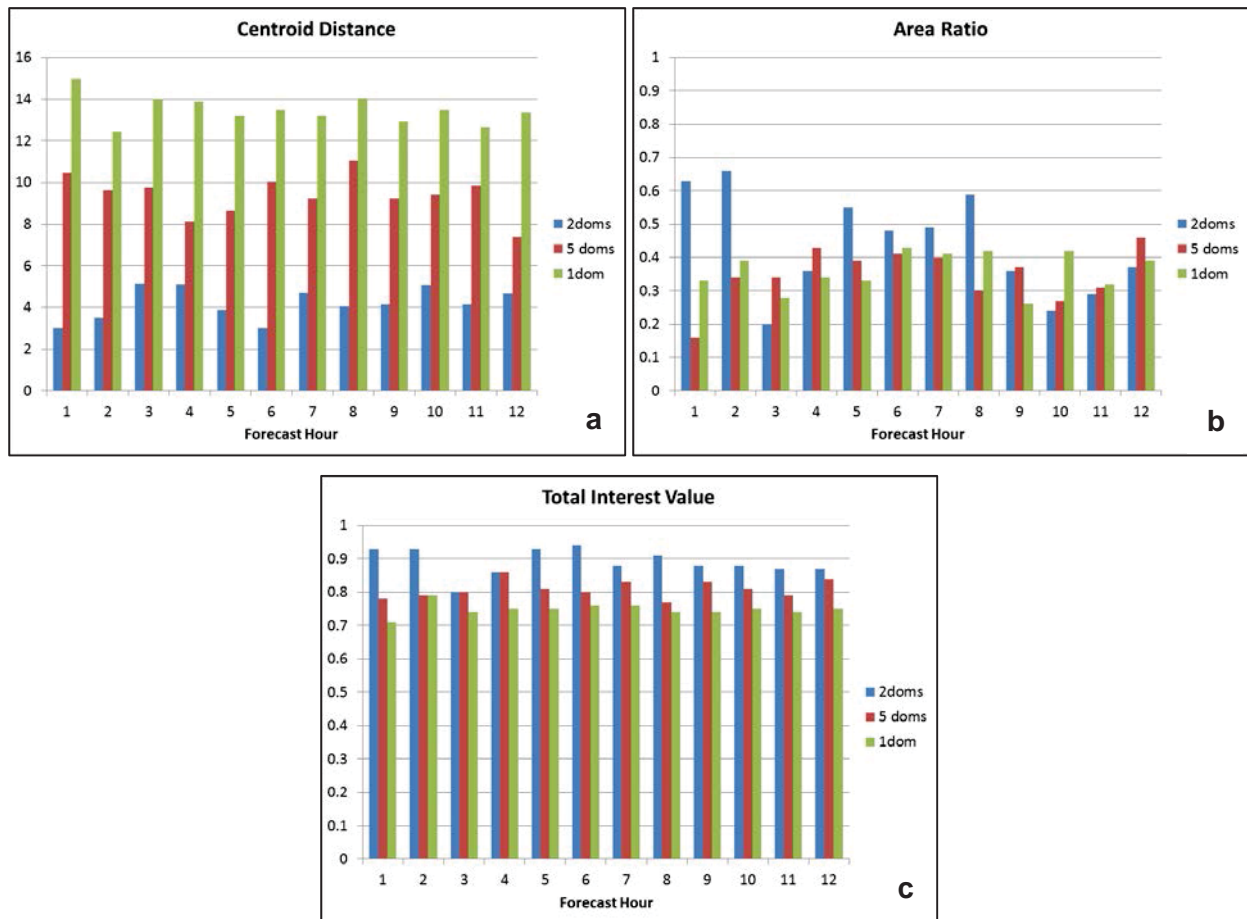


Figure 11. Chart of the average hourly a) centroid distance (km), b) area ratio, and c) total interest value from the three GSI/WRF configurations for each hour of the 12-hour forecast over the entire POR at the ER.

3.4 WFF Results

The AMU validated model performance for WFF using forecasts from the grids described in section 2.3, where 2 doms references the nested 4-km outer and 1.33km inner domain (Figure 4) and 5 doms references the triple-nested 9-km outer, 3-km middle, and 1-km inner domain over WFF (Figure 3).

3.4.1 Surface Forecasts

The AMU validated the GSI/WRF forecasts with the local METAR and mesonet data. Figure 12 shows the ME for wind speed, wind direction, temperature, dewpoint temperature, and MSLP from the two GSI/WRF configurations averaged over each hour of each 12-hour forecast for the entire POR at WFF.

Overall, the ME results indicate that the triple-nest configuration performed better than the nested domain. The triple-nest configuration had the highest ME for wind speed, wind direction, temperature, and MSLP while the nested domain had the highest ME for dewpoint temperature.

Both model configurations over-predicted the wind speed throughout the forecast with a large increase in ME after the first forecast hour. However, the error for the triple-nest configuration was nearly 1.5 m/s less than that for the nested domain throughout the forecast. The same large increase after the first forecast hour in ME for wind direction was present in the nested domain with slightly decreasing values of ME after forecast hour 3, while the triple-nest configuration showed gradual increasing ME error values throughout the forecast period. The triple-nest configuration had lower ME values than the nested domain with differences in ME of approximately 15 to 30 degrees. ME values for temperature were nearly the same for both configurations during the first five forecast hours, after which the triple-nest configuration outperformed the nested domain with ME values of nearly 0. The triple-nest configuration consistently forecasted dewpoint temperature values that were too cool, while the nested domain was too cool during the first 5 hours and then too warm after that. Both configurations followed the same ME trend for MSLP with pressures that were initially too low and then too high in the latter part of the forecasts.

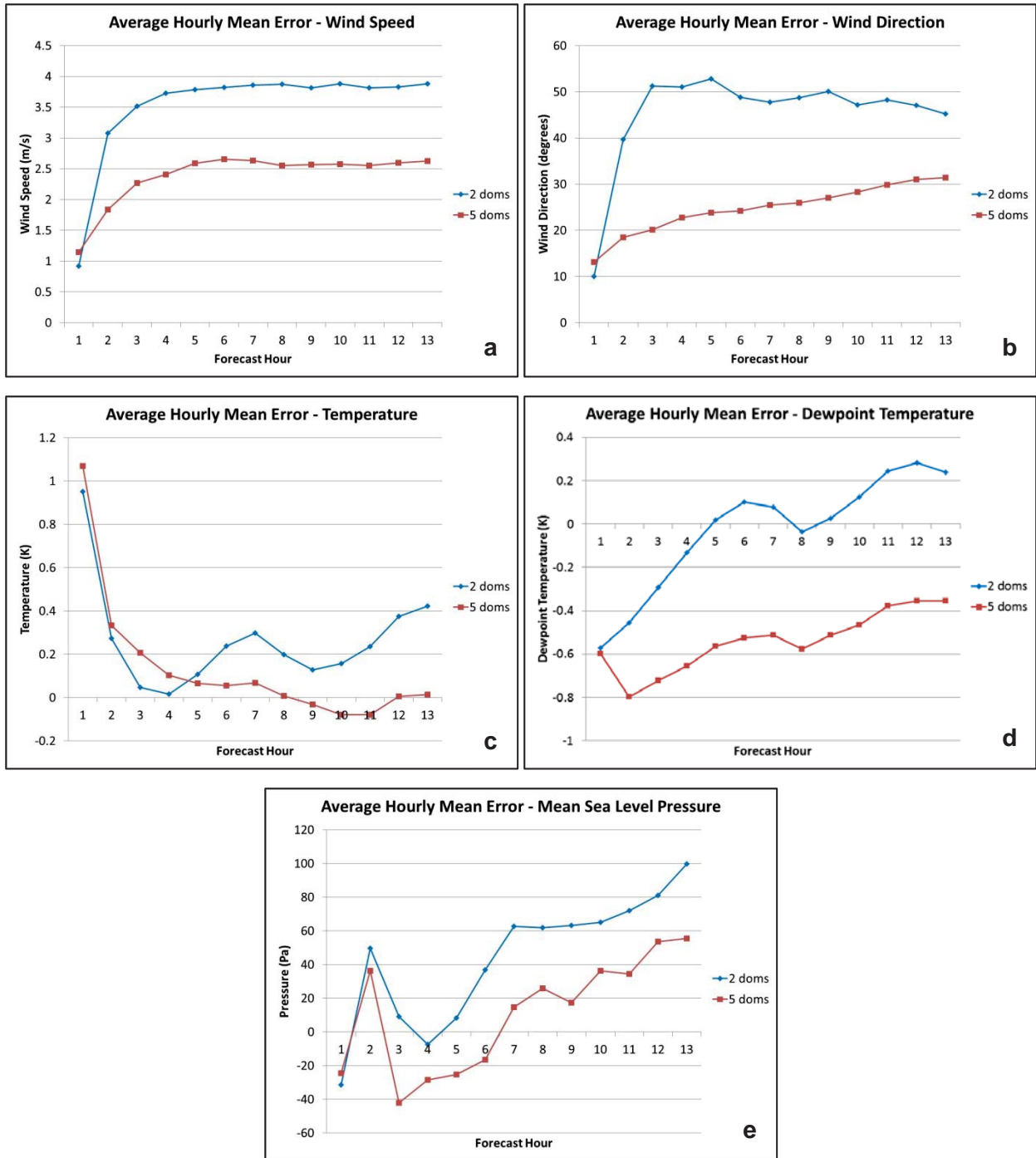


Figure 12. Chart of the average hourly ME for the 12-hour forecast over the entire POR for a) wind speed, b) wind direction, c) temperature, d) dewpoint temperature, and e) MSLP from the two GSI/WRF configurations at WFF.

Similar to the ME, the RMSE results (Figure 13) indicate that the triple-nest configuration performed the best for all variables. The RMSE wind speed and direction charts are nearly identical to the ME error charts indicating that there were not any large outliers for forecasted wind speed or direction. The triple-nest configuration RMSE for temperature and dewpoint temperature was roughly 1.25 K lower than that for the nested domain throughout the forecasts. Except for

forecast hours 2 and 3, the triple-nest configuration outperformed the nested domain for MSLP with differences of approximately 60 Pa lower in the latter half of the forecasts.

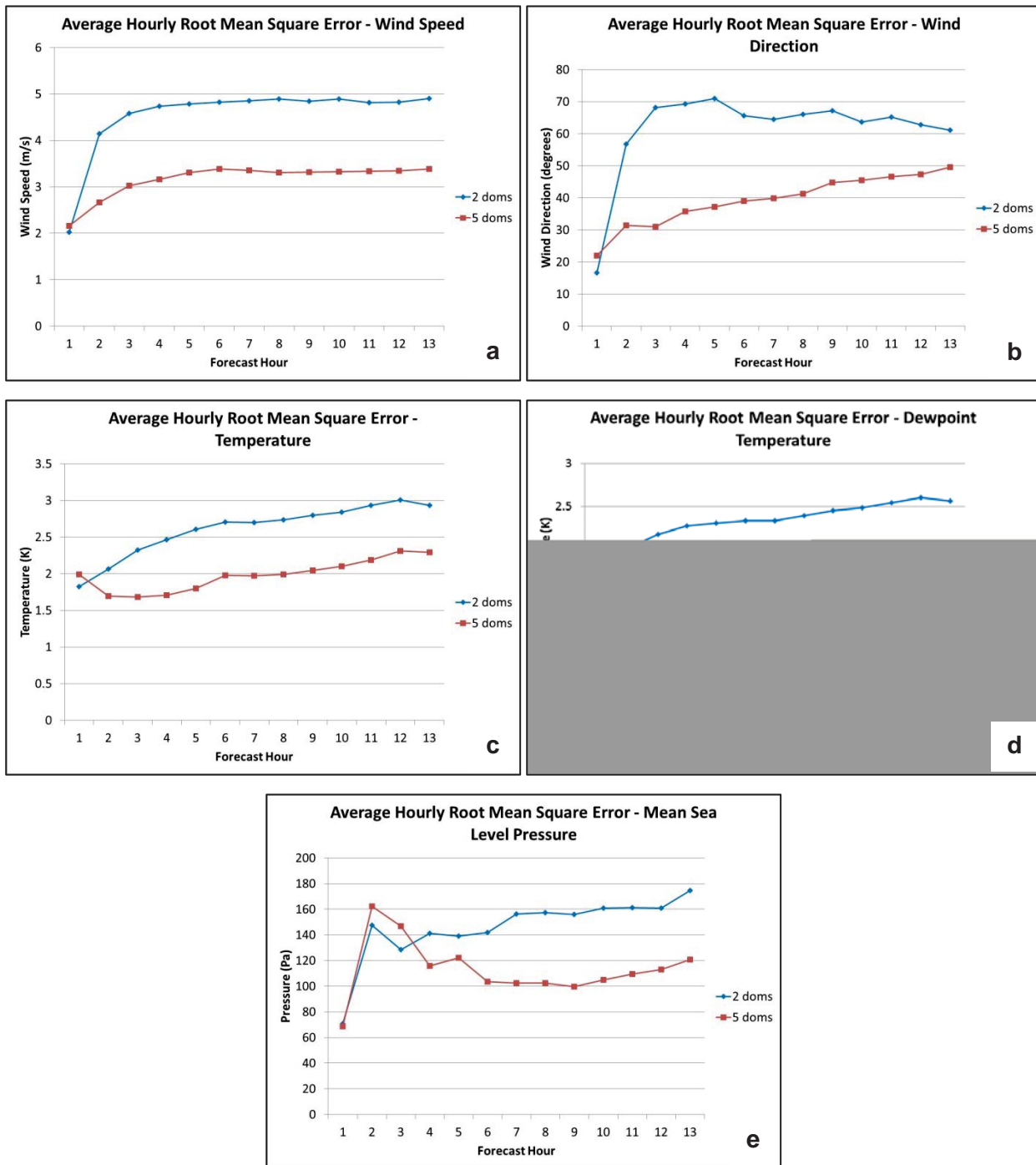


Figure 13. Chart of the average hourly RMSE for the 12-hour forecast over the entire POR for a) wind speed, b) wind direction, c) temperature, d) dewpoint temperature, and e) MSLP from the two GSI/WRF configurations at WFF.

The results from the PCC calculation (Figure 14) indicate that the triple-nest configuration again outperformed the nested domain for wind speed, temperature, dewpoint temperature, and MSLP. The PCC for the triple-nest configuration for wind speed and temperature was approximately 0.05 to 0.1 higher than the nested domain throughout the forecast. The PCC for dewpoint temperature was 0.2 to 0.3 higher for the triple-nest configuration and was up to 0.1 higher through forecast hours 4 to 11 than the nested domain for MSLP. It is interesting to note that the highest PCC values for WFF were nearly double that of the ER. During the summer and fall, different systems drive the local weather at each range. There are more synoptic systems that influence the weather over the WFF during summer and fall while in the summer, the weather over the ER is locally driven by mesoscale phenomena. In general, models will perform better when the local weather is driven by larger-scale synoptic systems. Therefore, it is expected that the GSI/WRF system performed better for WFF than for the ER during the POR.

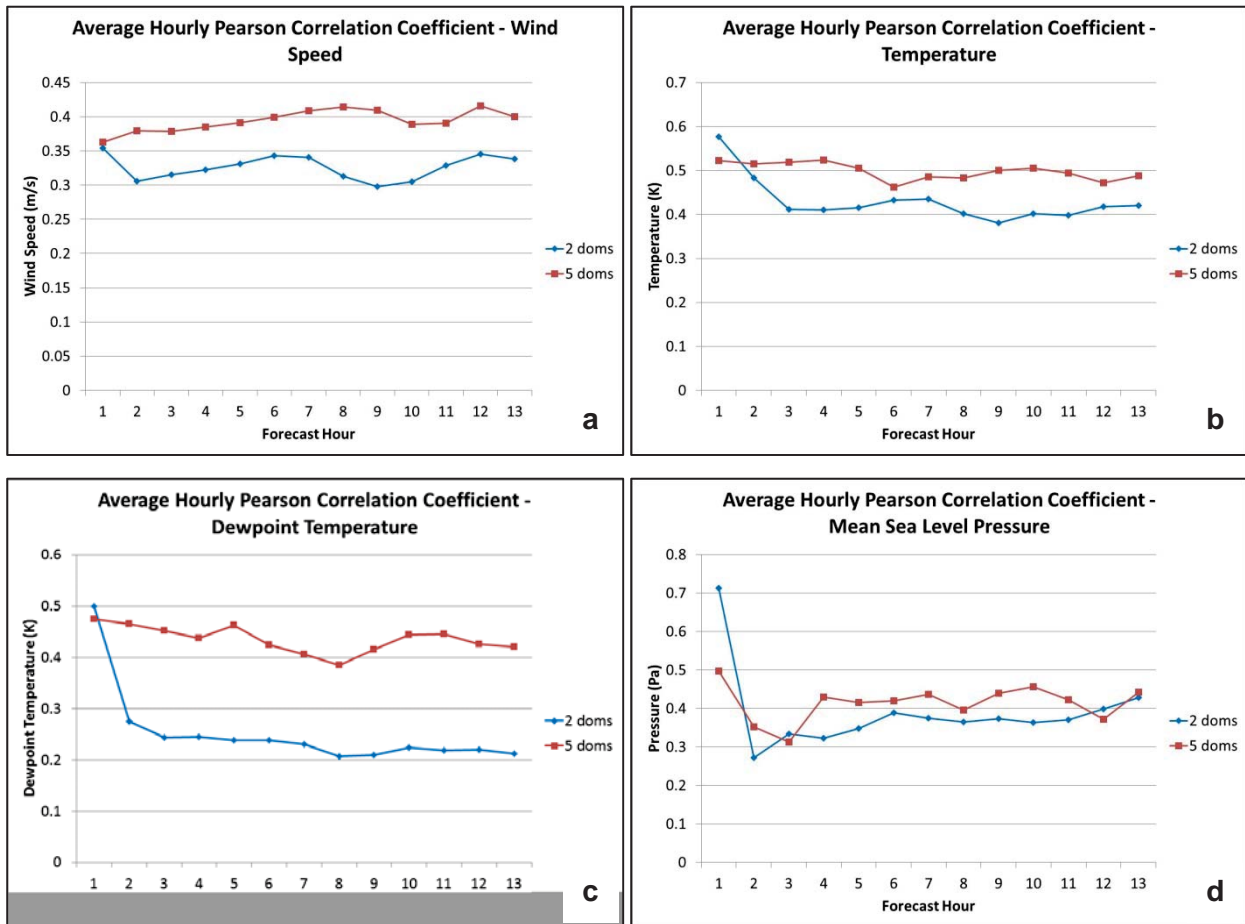


Figure 14. Chart of the average hourly PCC for the 12-hour forecast over the entire POR for a) wind speed, b) temperature, c) dewpoint temperature, and d) MSLP from the two GSI/WRF configurations at WFF.

3.4.2 Precipitation Forecasts

The AMU compared precipitation forecasts from both model configurations to determine performance differences. One-hour forecast accumulated rainfall for each hour of each of the 12-hour forecasts was compared to the one-hour accumulation of observed rain using the NCEP Stage-IV analysis data for each day during the POR. The POR summary statistics for each hour of the forecast of centroid distance, area ratio, and interest function from the MODE software are shown in Figure 15. The centroid distance (km) results indicate that forecasts from both configurations were very similar in their ability to match the location of the observed precipitation throughout the forecasts. However, the triple-nest configuration did slightly better in predicting the precipitation location. The area ratio results indicate that accumulated precipitation for the triple-nest configuration matched the areal coverage of observed precipitation more closely, although the results were comparable. Total interest values were very similar for both configurations with values near 0.8. Overall, the triple nest configuration very slightly outperformed the nested domain.

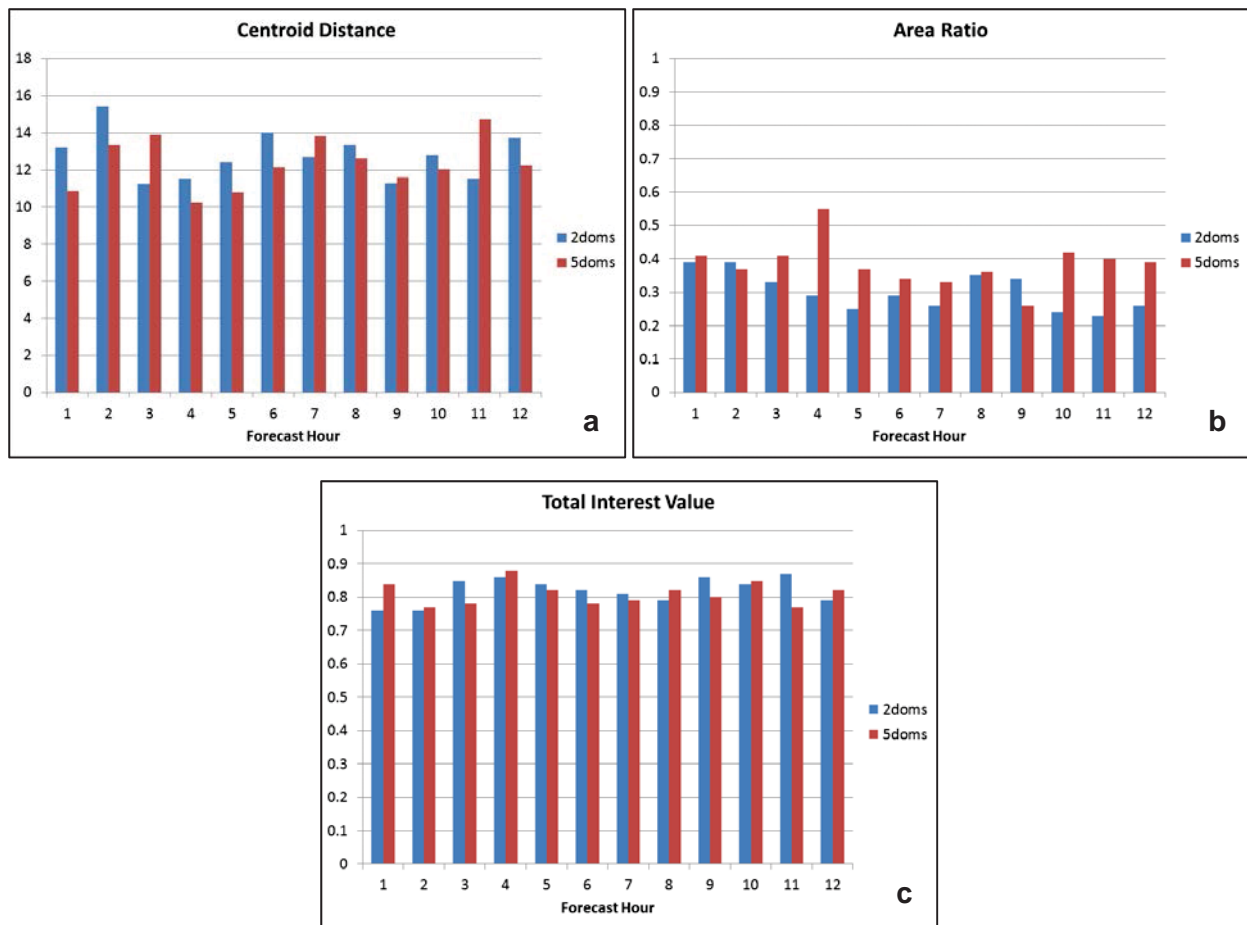


Figure 15. Chart of the average hourly a) centroid distance (km), b) area ratio, and c) total interest value from the two GSI/WRF configurations for each hour of the 12-hour forecast over the entire POR at WFF.

4 Conclusions and Future Work

This report summarizes the findings from the AMU task to determine a recommended local DA and numerical forecast model design optimized for the ER and WFF to support space launch activities and for local weather forecasting challenges at each range. The AMU ran the GSI/WRF model system over part of the summer and fall seasons for each range while varying grid resolutions on which the DA was run and varying the nesting configurations to determine the impact on model skill. In general for both the ER and WFF, the triple-nest configuration outperformed the other configurations. However, although the results for the ER indicate that the triple-nest configuration performed best for most variables as evidenced by the ME, RMSE, and PCC, the nested configuration did the best in predicting precipitation for the ER. Summertime convection over the ER is an important meteorological variable to predict and, for this reason, it is the AMU's recommendation to use either the nested or triple-nest configuration as the optimal model configuration for the ER. The triple-nest configuration performed the best for nearly all variables at WFF. Wind, temperature, and convective activity forecasts during the fall and spring seasons pose the most difficulties for forecasters at WFF. Therefore, it is the AMU's opinion that the triple-nested domain is the optimal model configuration for WFF.

The AMU has been tasked with a follow-on modeling effort to:

- Port GSI/WRF code from the AMU developmental cluster to the AMU real-time cluster and to run every three hours,
- Display real-time output of the GSI/WRF cycled runs on the AMU's AWIPS II workstations,
- Work with SPoRT to determine if the GSI/WRF system can be run in a rapid-refresh mode. If so, determine the time-frame to set up the rapid-refresh system and implement if possible within the time-frame of this task, and
- Explore ensemble modeling using the WRF model and determine the level of effort and time-frame to set up an ensemble modeling system.

This follow-on task will benefit operations by providing high spatial and time resolution forecasts from a model tuned specifically for their location. It will also continue to improve the local model by incorporating techniques that have been shown to enhance model performance.

References

- Davis, C., B. Brown, and R. Bullock, 2006: Object-based verification of precipitation forecasts. Part I: Methods and application to mesoscale rain areas. *Mon. Wea. Rev.*, **134**, 1772–1784.
- Kleist, D. T., D. F. Parrish, J. C. Derber, R. Treadon, W. Wu, S. Lord, 2009: Introduction of the GSI into the NCEP Global Data Assimilation System. *Wea. Forecasting*, **24**, 1691–1705.
- Lin, Y. and K. E. Mitchell, 2005: The NCEP Stage II/IV hourly precipitation analyses: development and applications. Preprints, *19th Conf. on Hydrology*, San Diego, CA, Amer. Meteor. Soc., P1.2. [Available online at ams.confex.com/ams/Annual2005/techprogram/paper_83847.htm.]
- Wang, Xuguang, 2010: Incorporating ensemble covariance in the Gridpoint Statistical Interpolation variational minimization: A mathematical framework. *Mon. Wea. Rev.*, **138**, 2990–2995.
- Watson, L., 2013: Range-specific High-resolution Mesoscale Model Setup. NASA Contractor Report CR-2013-217911, Kennedy Space Center, FL, 41 pp. [Available from ENSCO, Inc., 1980 N. Atlantic Ave., Suite 830, Cocoa Beach, FL, 32931 and online at <http://science.ksc.nasa.gov/amu/final-reports/range-specific-hi-res-model-setup.pdf>.]

List of Acronyms

45 WS	45th Weather Squadron	MSLP	Mean Sea-Level Pressure
AMU	Applied Meteorology Unit	NAM	North American Mesoscale
ARW	Advanced Research WRF	NCAR	National Center for Atmospheric Research
AWIPS	Advanced Weather Interactive Processing System	NCEP	National Centers for Environmental Prediction
CCAFS	Cape Canaveral Air Force Station	NMM	Non-hydrostatic Mesoscale Model
DA	Data Assimilation	PBL	Planetary Boundary Layer
ER	Eastern Range	PCC	Pearson Correlation Coefficient
GSI	Gridpoint Statistical Interpolation	POR	Period of Record
KSC	Kennedy Space Center	RMSE	Root Mean Square Error
LIS	Land Information System	RAP	Rapid Refresh
MADIS	Meteorological Assimilation Data Ingest System	SPoRT	Short-term Prediction Research and Transition Center
ME	Mean Error	SST	Sea Surface Temperature
MET	Model Evaluation Tools	WFF	Wallops Flight Facility
METAR	Meteorological Aerodrome Report	WRF	Weather Research and Forecasting
MODE	Method for Object-Based Diagnostic Evaluation	YSU	Yonsei University

NOTICE

Mention of a copyrighted, trademarked or proprietary product, service, or document does not constitute endorsement thereof by the author, ENSCO Inc., the AMU, the National Aeronautics and Space Administration, or the United States Government. Any such mention is solely for the purpose of fully informing the reader of the resources used to conduct the work reported herein.